Modulation of Turbulence Energy by Longitudinal Rolls in an Unstable Planetary Boundary Layer[1]

MARGARET A. LEMONE

National Center for Atmospheric Research,[2] Boulder, Colo. 80303

(Manuscript received 12 December 1975, in revised form 19 March 1976)

ABSTRACT

Horizontal roll vortices influence the distribution of turbulence, with turbulence variances and fluxes concentrated in regions of positive roll vertical velocity w_r. This "modulation" of turbulence can be explained simply in terms of the advection of turbulence-generating elements by rolls.

A budget equation is derived for the roll-modulated turbulence energy. Evaluations of various terms in the equation shows that the modulation of turbulence variance is accounted for primarily by a similar modulation in mechanical and buoyancy production near the surface and by vertical transport at higher levels (~100 m). Energy exchange between rolls and turbulence is relatively unimportant. That is, the rolls modulate turbulence energy mainly by redistributing turbulence and turbulence-producing elements, rather than by exchanging energy.

Similarly, it is shown that the exchange of energy between rolls and roll-modulated turbulence contributes considerably less to the energy equation of rolls than does the major term, buoyancy.

1. Introduction

When the wind is sufficiently high and heat flux not too strong, longitudinal rolls aligned approximately parallel to the mean wind seem to be the dominant form of secondary flow in the planetary boundary layer or convectively mixed layer. When there is sufficient moisture, cloud lines form in and above the part of the roll with upward vertical velocity. According to Kuettner (1971), the spacing between adjacent cloud lines (roll lateral dimension) is normally between about 2 and 8 km, and the lines can be up to 500 km in length. Similar lateral dimensions independent of cloud observations are reported by Konrad (1970) and LeMone (1973); and in most cases, the ratio of lateral to vertical dimension is from 2:1 to 4:1. This ratio is comparable to that predicted from theory both for thermally driven flow (e.g., Asai, 1970) and rolls formed from an instability in the Ekman spiral (e.g., Faller and Kaylor, 1966; Lilly, 1966; Brown, 1970). Observations show that kilometer-scale cells or eddies and smaller scale eddies (of order 200 m and smaller) are superimposed on the mean roll circulation.

LeMone (1973) found that both energy production from the mean shear and from buoyancy must be included to adequately describe the circulation of rolls in the atmosphere. The shape of the observed roll circulation matches well that predicted by Faller and Kaylor (1966), Lilly (1966) and Brown (1970), for rolls formed from inflectional instability in the Ekman spiral. The magnitude of the observed roll circulation was, however, up to 40% larger than the predicted value for rolls obtaining energy from wind shear alone [see Faller and Kaylor (1966) or Brown (1970)]. It was found that the difference was most likely the result of the large contribution of buoyancy to the observed roll energy. The energy exchanged between rolls and smaller scale motions and the importance of this exchange to the roll energy budget were not, however, discussed.

It will be shown here, with data from aircraft flying normal to roll axes, that the smaller scale turbulence in a roll is systematically concentrated in regions of positive roll vertical velocity. This is similar to the relationship between large- and small-scale turbulent motions documented with tower data by Haugen *et al.* (1971) and Holland (1973). Since the variation of turbulence across the roll is systematic, it will be referred to as *modulated*. This modulation indicates an interaction and possibly an exchange of energy between the rolls and turbulence.

Here the modulation of turbulence by rolls is described and then related to the energetics of the mean roll circulation. Data from the NOAA DC-6 and the NCAR DeHavilland Buffalo aircraft are filtered and composited, as described in LeMone (1973), to determine the amplitude and phase of the turbulence modulation with respect to the roll circulation. The

[1] Contribution No. 355, University of Washington, Seattle. This paper is essentially a summary of the second half of the author's Ph.D. dissertation.

[2] The National Center for Atmospheric Research is sponsored by the National Science Foundation.

mean roll structure is assumed to be like that measured with the WKY-TV tower instrumented and operated by the National Severe Storms Laboratory and described in LeMone (1973).

The processes whereby the two scales exchange energy are described by terms appearing in both the roll energy equation from LeMone (1973) and the roll-modulated energy equation derived here. These energy exchange terms are evaluated to determine the energy gain or loss to the rolls as a result of this modulation.

The generality of the reported results is limited by the range of conditions under which the measurements were taken, and by the number of rolls observed in each case. The computations and conclusions are based on four sets of aircraft data, using knowledge of the roll vertical structure gained primarily from four sets of tower data. These data were collected in conditions ranging from air-mass modification situations over Lake Michigan to a situation with steady trade winds and suppressed convection near Barbados during BOMEX (see Fleagle, 1972). Turbulence measurements are available from the aircraft only, and these were confined to the lower third of the roll. The number of rolls sensed at a given flight level was as small as 2 or 3.

2. Data acquisition and processing

a. Instrumentation

Roll wind, humidity and temperature fields were sensed with two aircraft—the NCAR Buffalo and the NOAA DC-6. Both aircraft have inertial platforms, which make possible measurements of wind fluctuations over the broad spectrum of wavelengths needed for this study. The Buffalo and DC-6 instrumentation systems are discussed in detail by Lenschow (1972) and Lilly and Lenschow (1974), and by Friedman *et al.* (1970), respectively. Here, they will be discussed only briefly.

Wind speed from the aircraft is computed by subtracting the aircraft motion with respect to the ground from the air velocity with respect to the aircraft. The air motion with respect to the Buffalo is measured with a fixed angle of attack vane, a fixed angle of sideslip vane, and a pitot tube. The temperature was sensed with a resistance wire (Rosemount model 102EAL), and humidity was determined by combining the temperature and static pressure measurements with atmospheric microwave refractive index measurements from a microwave refractometer borrowed from the Wave Propagation Laboratory (WPL) of NOAA, Boulder.

According to Lenschow (1972) the error in average windspeed is about 1 m s^{-1}. The errors in wind fluctuations are about 8% of the amplitude of lateral (normal to aircraft axis) wind velocities, and 2% of the amplitude of gusts along the aircraft axis, down to about 10 cm s^{-1}. The temperature is accurate to about 0.2 K, with a fluctuation error of the order of 0.03 K. The DC-6 system has similar characteristics, except that the slideslip angle was not measured.

However, in both cases, the sampling error is probably greater than the instrumental error. Since rolls have typical wavelengths ranging from 2 to 8 km, the number of rolls encountered by either aircraft on a typical (5 min or 23 km) crosswind run would be from 3 to 10.

b. Flight plans

The Buffalo aircraft measurements used here are from two field programs. The first set of data is from a tower-aircraft comparison flight conducted by NCAR and NOAA WPL at the NOAA meteorological tower near Haswell, Colo. In this case, a 23 km box centered at the tower was flown at an average altitude of 90 m. Due to topographical variation, however, the aircraft was between 45 and 170 m above the ground during measurements. Since the downwind flights were not of sufficient length to determine roll orientation, the rolls were assumed parallel to the surface wind, which on this day was from the north. From previous statistics on roll orientation with respect to the wind in neutral to slightly unstable planetary boundary layers, this leads to a maximum 10°–15° orientation error.

Two of the data sets examined here were collected by the Buffalo aircraft over Lake Michigan during a cold air outbreak investigation in November 1970. L-shaped patterns 23 km on a side were flown along and normal to the wind at levels between 30 and 320 m above the surface to measure detailed convective structure. Roughly alongwind runs across the lake provided data for roll orientation, and aircraft soundings provided temperature and humidity profiles. The data sampling rate was 8 per second but effectively reduced to 4 per second by block averaging. This sampling rate was still sufficient to measure most of the energy-carrying eddies at flight altitudes, with the short-wavelength cutoff at about 35 m.

The data for the fourth case examined here were gathered on a suppressed day during BOMEX, in a flight pattern similar to the other three. Here the DC-6 flew legs 28 km in length along and normal to the wind at 18, 46 and 150 m above the surface. The rolls were again assumed parallel to the wind. The data were digitized at 20 per second after low-pass filtering with a cutoff at 4.5 Hz.

c. Selection of cases for study

Before extensive analysis, traces of horizontal and vertical velocity were examined for evidence of rolls. In the lower part of the roll there is about a 90° phase lag between the wind component normal to the mean vector and the vertical velocity. For an aircraft flying crosswind at 70 m s^{-1}, rolls with typical wavelengths of 2–6 km appear as fluctuations with a period between 30 and 70 s. On downwind runs almost parallel to the rolls, the roll periods were 5–10 min.

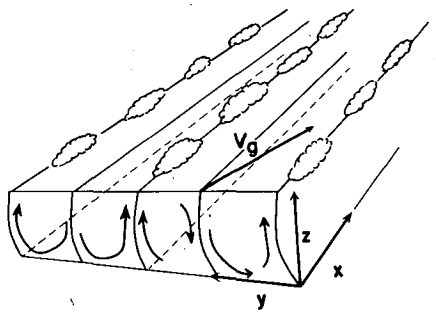

FIG. 1. Roll coordinate system.

At the time of analysis, horizontal wind data were not available from the DC-6. Hence, cloud pictures were examined for evidence of roll occurrence.

d. Filtering and compositing

Higher frequencies were separated from those in the roll-frequency band with a low-pass Graham filter (Graham, 1963). For an infinite number of weights, the response function $R(f)$ is given by (a list of symbols is given in an appendix)

$$R(f)=\begin{cases}1, & f<f_c\\ 0, & f\geqslant f_t\\ \frac{1}{2}\left\{1+\cos\left[\dfrac{(f-f_c)\pi}{f-f_t}\right]\right\}, & f_c\leqslant f<f_t\end{cases} \tag{2.1}$$

For a finite number of weights the response function overshoots at f_c and f_t, oscillating around $R=1$ for $f<f_c$, and about $R=0$ for $f\geqslant f_t$.

In each case, the numerical values of f_c and f_t were determined after examining the temperature, humidity and velocity spectra. Error in response was reduced by having the response fall off in the spectral gap, and making f_c-f_t and the number of weights large.

Roll-band frequencies were isolated by the above procedure after eliminating the linear trend from the raw data, and are denoted by the subscript l. Fluctuations of higher frequency are denoted by primes and are found from equations of the form

$$q'=q-\bar{Q}-q_l, \tag{2.2}$$

where q is any quantity and $\bar{Q}$ its average over a complete flight leg.

Before and after filtering, data are detrended by linear regression over an integral number of rolls. Fluxes and variances are computed from detrended data using the eddy correlation technique.

In order to isolate two-dimensional rolls from other kilometer-scale fluctuations, the filtered data for several rolls are averaged to form a composite roll for that leg. Assuming that the rolls are uniform and that their length is much greater than their width, this approximates averaging in the longitudianl direction. Averaging was done at 33 points per roll wavelength. The points were selected primarily on the basis of low-frequency vertical velocity maxima, with the first and 33rd points corresponding to vertical velocity maxima, and the 17th point corresponding roughly to the vertical velocity minimum, with the remaining points evenly spaced between. Hence, for example, T_{ri} (the composite roll temperature at point i, based on a composite of n rolls) is given by

$$T_{ri}=\frac{1}{n}\sum_{j=1}^{n}T_{lij}. \tag{2.3}$$

e. Determination of the Obukhov length L

In the notation used in this paper, the Obukhov length is given by

$$L=\frac{-\bar{T}_0[\overline{(u_l+u')(w_l+w')}\,|_0{}^2+\overline{(v_l+v')(w_l+w')}\,|_0{}^2]^{\frac{3}{2}}}{gk\overline{(w_l+w')(T_l+T')}\,|_0}.$$

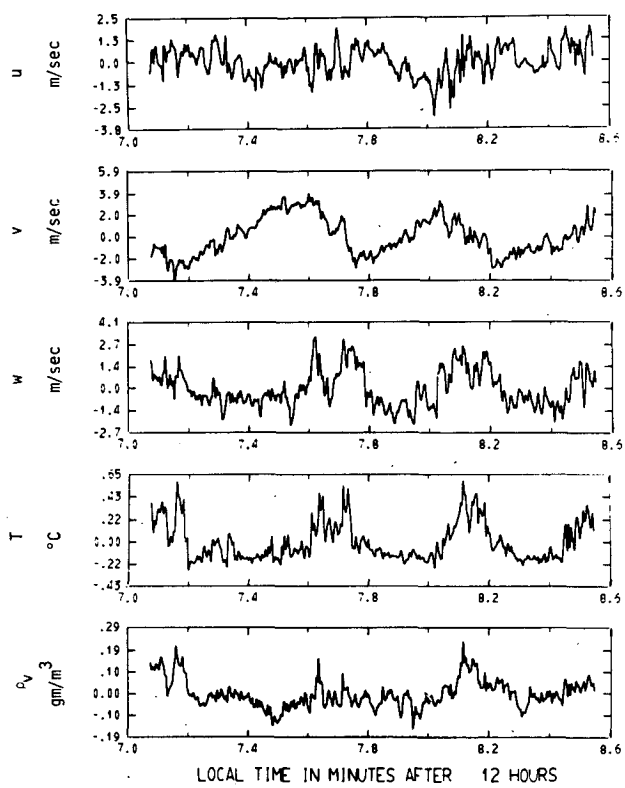

FIG. 2a. Fluctuations of wind components u, v and w (roll coordinates), temperature T, and absolute humidity ρ_v, as recorded by the NCAR Buffalo aircraft flying normal to well-organized rolls 175 m above the surface. Airspeed is 70 m s^{-1}; Obukhov length L, -100 m; inversion height, 1000 m; Haswell, Colo., 1 October 1970.

The zero-subscripted values are surface values, and are based on profiles extrapolated to the surface. The von Kármán constant k is assumed equal to 0.4.

3. Description of the modulation of energy by rolls

a. The partition of energy between rolls and turbulence

Fig. 2a shows traces of temperature, humidity, and velocity components u, v and w as measured by the Buffalo aircraft flying crosswind through rolls on 1 October 1970, near Haswell, Colo. The wind components are with respect to a right-hand roll coordinate system (Fig. 1), with the x axis along the roll axis, pointing downwind. Trends and means have been removed. The aircraft was flying at roughly 70 m s^{-1} at an altitude of 175 m. The rolls appear in Fig. 2 as 30 s (2.1 km) oscillations in u, v, w, T and ρ_v. Note the near 90° phase lag between v and w, indicating that at least part of the vertical velocity is explained by convergence in v. (If the rolls are strictly two-dimensional, of course, all the vertical velocity would have to result from convergence in v.) Superimposed on the rolls are higher

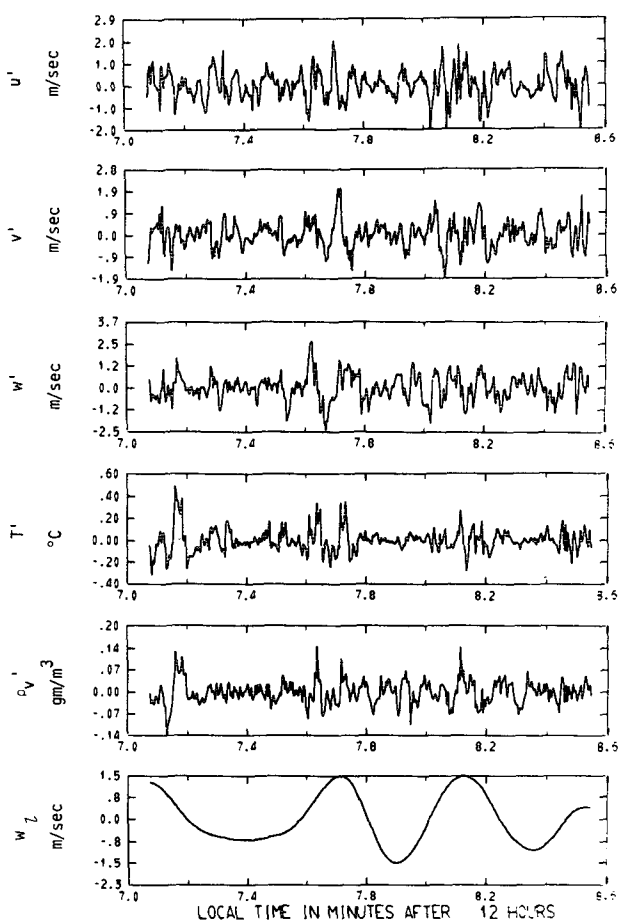

FIG. 2b. As in Fig. 2a except for turbulence velocity u', v' and w' (roll coordinates), temperature T, and absolute humidity ρ_v. The role-scale vertical velocity w_l appears in the lowest frame.

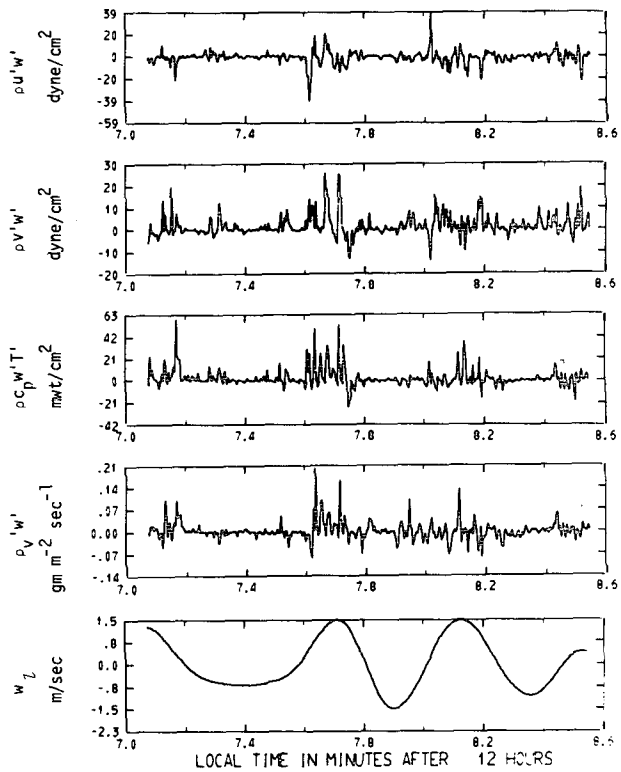

FIG. 2c. Turbulence fluxes of u and v momentum, heat and absolute humidity for same period as Fig. 2a. The role-scale vertical velocity w_l appears in the lowest frame.

frequency oscillations, concentrated in regions of positive roll vertical velocity. The relation of u to the rolls, if any, is less obvious.

How meaningful is the division of energy between turbulence and rolls? Fig. 3 shows spectra of u, v, w, T and ρ_v, for a 5 min (21 km) leg which includes the measurements in Fig. 2. Confirming the impression from Fig. 2, the vertical velocity and temperature have two distinct peaks: one at 0.03 Hz (2.1 km) and one at 0.3 Hz (210 m). On the basis of the 90° phase difference between low frequency v and w, the 2.1 km peak can be identified as due to rolls. The 210 m peak, which occurs in u as well as w and T, can be associated with plumes and less organized turbulence. Based on an examination of the time traces of height u and ρ_v, the 0.012 Hz spectral peak in u and ρ_v seems to be related to the height of the aircraft above the terrain.

From Fig. 4, the composite roll energy accounts for a significant part of the low-frequency energy. Recall from Section 2 that the roll temperature variance T_r^2, for example, is found by averaging T_l at corresponding points over several rolls. Hence the hatched area in the figure could reflect the presence of some rolls with stronger circulation, kilometer-scale cells superimposed on the rolls as reported by Konrad (1970), or other irregularities. These three categories will be collectively referred to as "kilometer-scale turbulence."

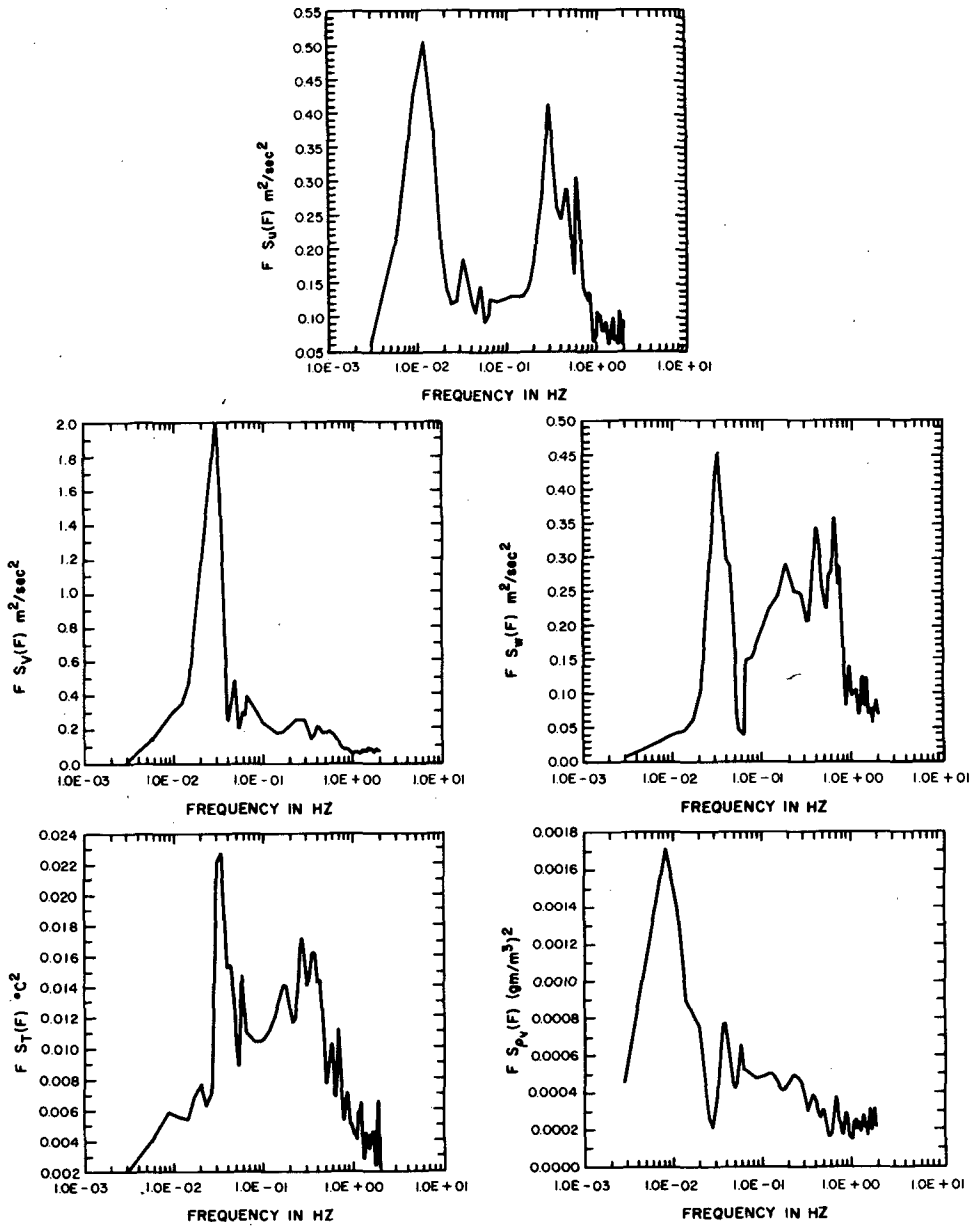

FIG. 3. Spectra of velocity components of u, v and w (roll coordinates), temperature T, and absolute humidity ρ_v from the NCAR Buffalo aircraft flying normal to roll axis at 100—170 m above undulating terrain, near the Haswell, Colo., meteorological tower. Airspeed 70 m s^{-1}. Spectra are computed from 5 min of data, a portion of which appears in Fig. 2a.

For the two cases in Fig. 5, the rolls account for more than half of the heat transport in the convectively mixed layer at heights greater than $-L$.

b. A qualitative discussion of the modulation

Based on the above example, the fluctuations of temperature, humidity and wind can be divided into three categories—rolls, kilometer-scale turbulence, and turbulence of smaller scale. The smaller scale turbulence, for the cases under study, had its maximum energy for crosswind wavelengths of the order of a few hundred meters. Although interactions between all these scales occur, only the simplest interaction, that between idealized two-dimensional rolls and the smaller scale turbulence, will be discussed here.

Roll-modulated turbulence variance and flux could be described in terms of block averages of higher frequency data at several points along the roll. We find it more convenient, however, to use the filter-composite scheme of Section 2 to obtain smoothly-varying curves

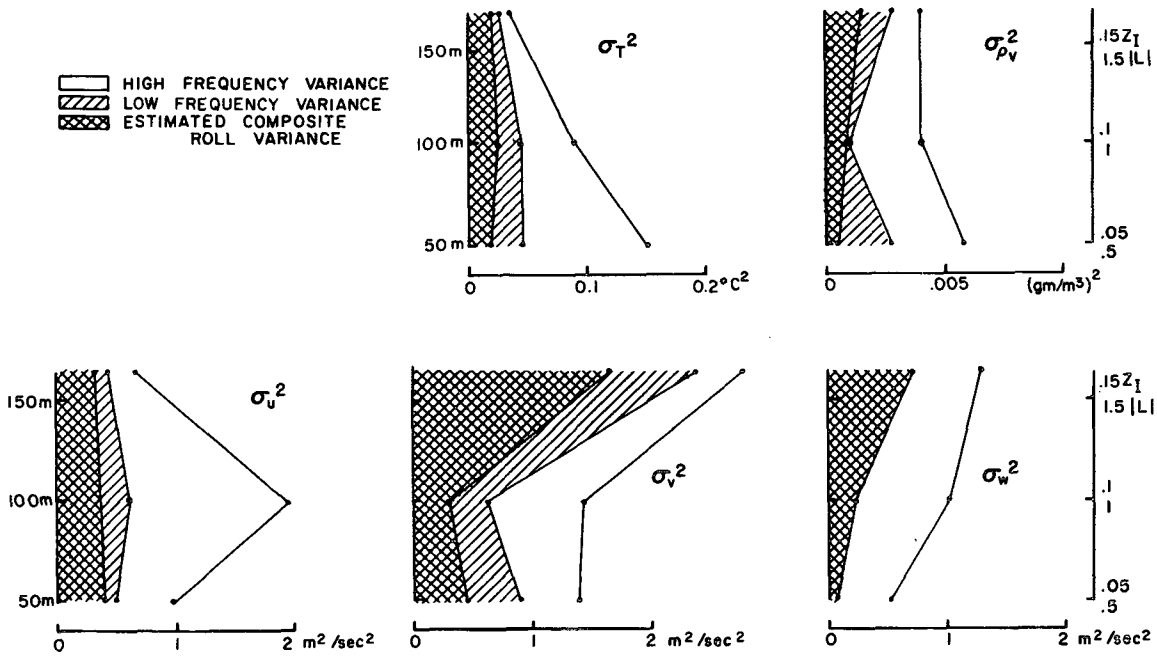

FIG. 4. High-frequency, low-frequency, and roll variance as a function of height for Haswell, Colo., 1 October 1970 data, after removal of mean. $|L| = 100$ m, $z_I = 1$ km.

of roll-modulated variance $(a'^2)_r$ or flux $(a'b')_r$. An extra advantage is that these quantities can be directly used in the equations to be derived in the next section.

Roll-modulated fluxes and variances of u, v, w, T and ρ_v associated with smaller-scale turbulence are plotted for several levels for two cases in Figs. 6, 7 (1 October, Haswell) and 8 (11 May, BOMEX). Note that the fluxes and variances are concentrated in regions of positive roll vertical velocity. The large flux regions exhibit the characteristics of the turbulent "bursts" observed by Haugen *et al.* (1971) in moderate to high wind speeds (>6 m s^{-1} at 22.6 m) with marked increase of stress (negative momentum flux divided by air density) with height and large positive heat flux. Discontinuities occur in curves which were composited using the vertical velocity minima as end points for each roll instead of the maxima.

The modulation of turbulence energy by rolls can be most simply viewed as the result of concentration of turbulence-producing eddies by the roll circulation. That is, the turbulent eddies near the surface are transported horizontally by the roll lateral velocity (v_r) into roll positive vertical velocity regions where upward growth or movement is favored.

This simple picture is complicated somewhat by the presence of other less passive structures. A strong plume, for example, may be able to penetrate upward in the negative vertical velocity region, particularly in the lower levels of the mixed layer. Further, the observed rolls can coexist with convection cells of comparable scale, as observed on radar by Konrad (1970) and in tower data by LeMone (1973). In this case, the cells would also contribute to the modulation of smaller scale turbulence. However, these irregularities tend to disappear when the turbulence modulation is averaged over a large number of rolls. In Fig. 8, which is based on

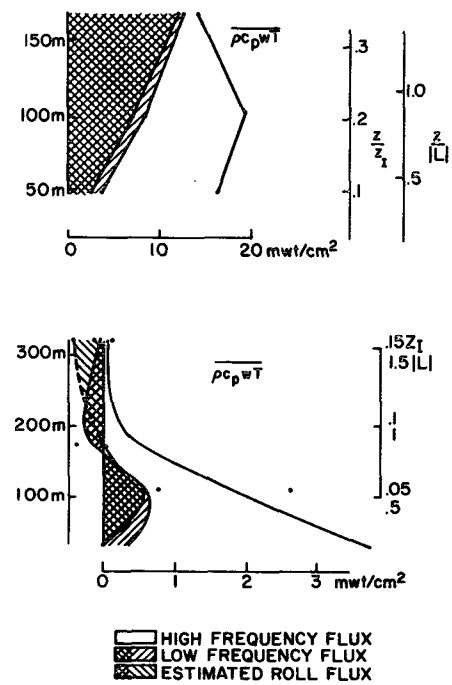

FIG. 5. High-frequency, low-frequency, and roll fluxes as a function of height, for (top) Haswell, Colo., 1 October 1970, and (bottom) Lake Michigan, 5 November 1970.

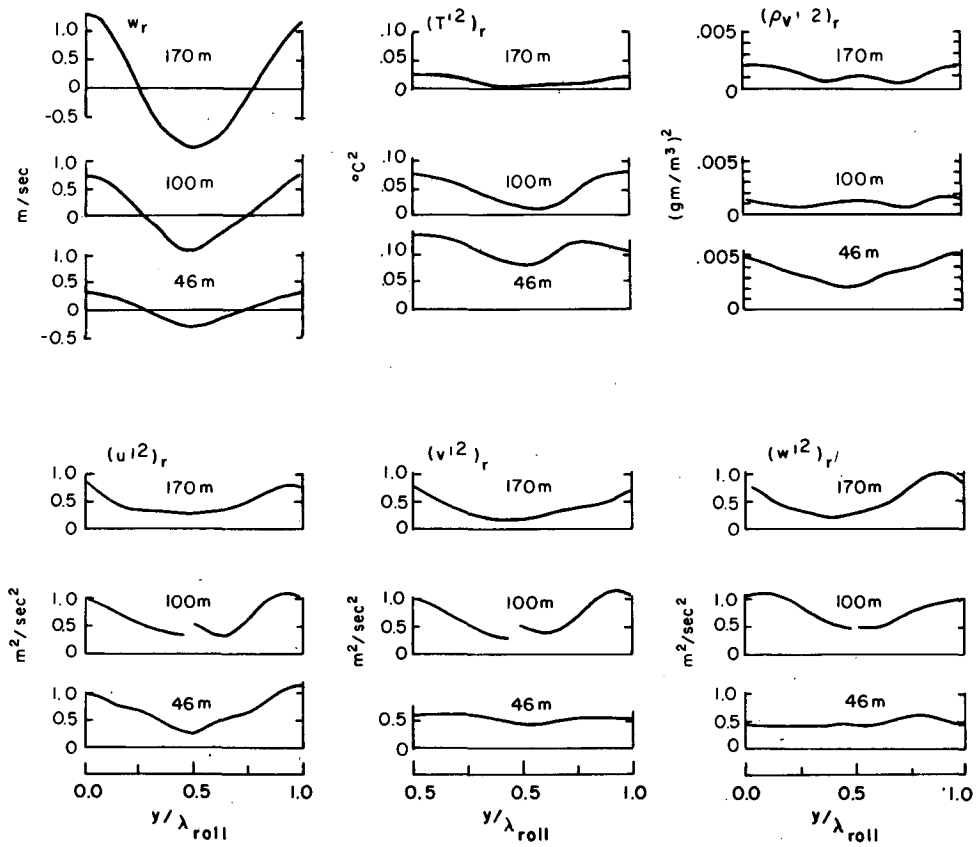

FIG. 6. Variation of turbulent variance across roll over Haswell, Colo., 1 October 1970. Obukhov length, −100 m; inversion height, 1 km. Composite curves for 46, 110 and 170 m are based on 6, 3 and 3 rolls, respectively. Maximum roll vertical velocity w_r for individual and composite curves is at $y=0$ and $y=1$; minimum w_r at $y=0.5$. "Turbulent" excludes motions of roll scale and larger.

a composite of about 70 rolls at each level, the turbulence modulation is sinusoidal.

4. The roll-turbulence interaction equations

In order to determine precisely the energy exchanges related to the interactions just described, we will derive the equations for roll kinetic energy and roll-modulated turbulence kinetic energy. The derivation is analogous to that used in LeMone (1973).

The Navier–Stokes equation for a fluid in a coordinate system rotating with an angular velocity Ω can be written

$$\frac{d\mathbf{v}}{dt} = -2\boldsymbol{\Omega}\times\mathbf{v}+\nu\nabla^2\mathbf{v}-g\mathbf{k}-\frac{1}{\rho}\nabla p, \tag{4.1}$$

where the constant coefficient ν is the coefficient of molecular viscosity. Eddy exchange terms will be specified in terms of turbulent variables. It is assumed that the effects of moisture in the liquid phase are negligible. We also use the incompressible equation of continuity

$$\nabla\cdot\mathbf{v}=0. \tag{4.2}$$

Consider motion of three scales: the synoptic scale, denoted by capitalization and an overbar; the roll scale, denoted by the subscript l, and the turbulent scale, denoted by the prime. A quantity q is then represented by

$$q=\bar{Q}+q_l+q'. \tag{4.3}$$

Since the roll scale includes kilometer-scale turbulence as well as rolls,

$$q_l=q_r+q'', \tag{4.4}$$

where the double prime will be used to denote kilometer-scale structures or turbulence other than rolls. Note the similarity of these definitions to those in Section 2.

The roll-modulated turbulence kinetic energy, in the notation introduced in Section 2, is $(E')_r=\frac{1}{2}(u'^2+v'^2+w'^2)_r$. The derivation of the equation for the local time rate of change of this quantity, keeping in mind the precise meaning of this notation, is straightforward. First, we multiply the i, j, k components of (4.1) by $u'\mathbf{i}$, $v'\mathbf{j}$, $w'\mathbf{k}$, respectively. Then, the resulting equation is filtered, using an ideal low-pass filter whose response

function $R(f)$ is given by

$$R(f)=\begin{cases}1, & f\leqslant f_c\\ 0, & f>f_c\end{cases} \tag{4.5}$$

where the cutoff frequency f_c is greater than the roll frequency. [In actually processing the data to evaluate terms in this equation, we of course use the filter whose response is defined by (2.1).] After simplifying the resultant equation using (4.2) and (4.3), we have the equation for $(E')_l$:

$$\frac{\partial(E')_l}{\partial t}=-(u_i'u_j')_l\frac{\partial\bar{U}_i}{\partial x_j}+\frac{g}{\bar{T}_v}(w'T_v')_l-\epsilon_l-(u_i'u_j')_l\frac{\partial u_{il}}{\partial x_j}$$
$$-\left[\frac{1}{\bar{\rho}}\frac{\partial(p'u_i')_l}{\partial x_i}+\frac{\partial(E'u_i')_l}{\partial x_i}+u_{il}\frac{\partial(E')_l}{\partial x_i}\right]-\bar{U}_i\frac{\partial(E')_l}{\partial x_i}. \tag{4.6}$$

The i, j subscripted terms are written in the Einstein notation for compactness. The quantity ϵ_l is the turbulence dissipation, which varies across the roll.

These equations assume only the Boussinesq approximations, provided the Reynolds averaging assumptions apply, i.e., that

$$\left.\begin{aligned}(a_lb_lc')_l=(\bar{A}b_lc')_l=(\overline{A\bar{B}c'})_l=0\\ ((a'b')_lc_l)_l=(a'b')_lc_l\end{aligned}\right\}, \tag{4.7}$$

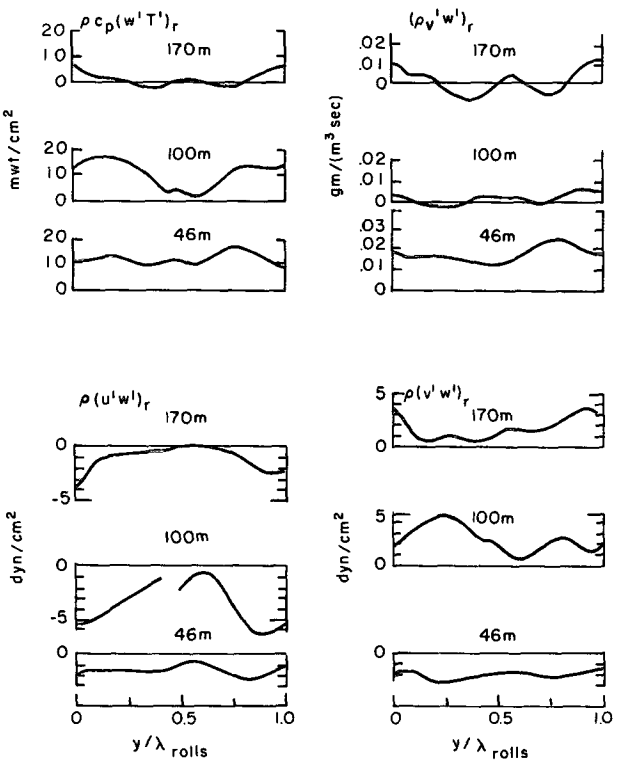

FIG. 7. Turbulent fluxes across roll, over Haswell, Colo., 1 October 1970. Otherwise as in legend to Fig. 6.

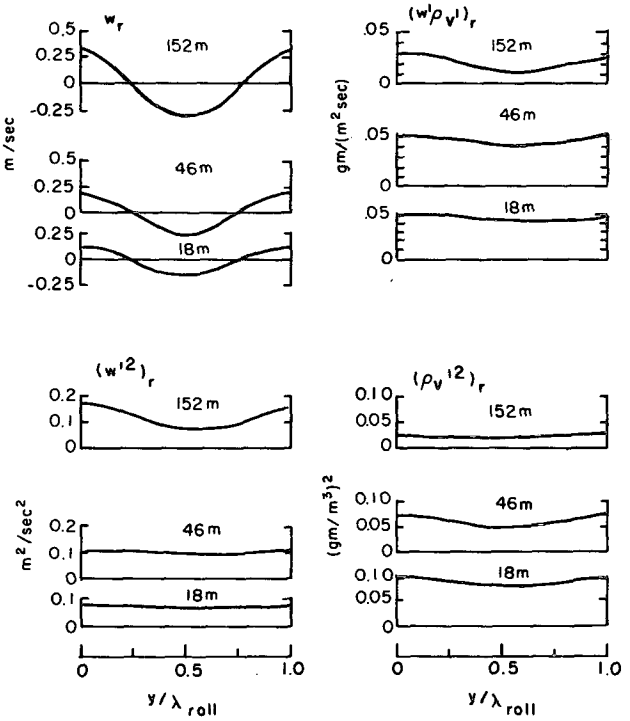

FIG. 8. Turbulent flux and variance across roll, from RFF DC-6, during BOMEX, 11 May 1969. Obukhov length, −60 m; inversion height, 6 km. Composite curves at 18, 46 and 152 m are based on 70, 67 and 70 rolls, respectively. Maximum w_r for individual and composite curves at $y=0$ and $y=1$, minimum w_r at $y=0.5$. "Turbulent" excludes motions of roll scale and larger.

where a, b, c represent any of u, v, w, T, ρ_v. It is well-known that relationships of the form (4.7) hold for ensemble averages, but these relationships are not generally true otherwise. Charnock (1957) showed that the Reynolds averaging assumptions apply for double correlations for the ideal filter [Eq. (4.5)], provided that there is a spectral gap between $f_c/2$ and $3f_c/2$, where f_c is the cutoff frequency for the filter. Similarly, (4.7) holds for a spectral gap between $f_c/3$ to $5f_c/3$.

Since the total filtering-compositing procedure which results in "r" quantities is something intermediate between the filter [Eq. (4.5)] and an ensemble average (see Section 2), note that (4.7) with subscript r is a better approximation than (4.7) in its original form.

In order to isolate roll-related fluctuations, Eq. (4.6) is spatially averaged in the x direction. This procedure is the same as using the compositing procedure[3] in Section 2, provided (i) there is no systematic variation of nonroll motions [the double prime terms] along the flight track (in these cases, always close to crosswind), such as convection cells aligned exactly along the flight

[3] That is, for each term T we form the integral

$$\frac{1}{x_2-x_1}\int_{x_1}^{x_2}T\,dx,$$

where x_2-x_1 is sufficiently large for a stable average.

track; (ii) there is a sufficient number of rolls; (iii) the rolls in the sample have a constant wavelength; and (iv) rolls are two-dimensional.

The rolls observed by LeMone (1973) had an extent in the x direction ten or more times their lateral dimension. For these rolls, we can write, to good approximation:

$$\left.\begin{aligned}\frac{\partial v_r}{\partial y}+\frac{\partial w_r}{\partial z}=-\frac{\partial u_r}{\partial x}=0\\ \frac{\partial(\ )_r}{\partial x}=0\end{aligned}\right\}. \tag{4.8}$$

Assuming that horizontal synoptic-scale gradients are small compared to those for roll and turbulence scales, and subsidence on the synoptic scale is negligible, we have

$$\bar{w}=\frac{\partial \bar{U}_i}{\partial x}=\frac{\partial \bar{U}_i}{\partial y}=0. \tag{4.9}$$

We average (4.6) in the x direction, and then simplify using (4.7)–(4.9), to obtain

$$\begin{aligned}\frac{\partial(E')_r}{\partial t}=&-(u'w')_r\frac{d\bar{U}}{dz}-(v'w')_r\frac{d\bar{V}}{dz}+\frac{g}{T_v}(w'T_v')_r-\epsilon_r\\ &-\left[(u_i'u_j')_l\frac{\partial u_i}{\partial x_j}\right]_r\\ &-\left[\frac{\partial}{\partial y}(p'v')_r+\frac{\partial}{\partial z}(p'w')_r\right.\\ &\left.+\left(u_{il}\frac{\partial(E')_l}{\partial x_i}\right)_r\right]-\bar{V}\frac{\partial(E')_r}{\partial y}.\end{aligned} \tag{4.10}$$

This equation is for the roll-modulated turbulence kinetic energy at a point. The first line of terms describes the contribution to the modulation by the local production and destruction of turbulence. This production of energy, as illustrated in Figs. 6–8, is concentrated in the positive vertical velocity regions of the rolls. Terms in the third and fourth lines represented energy transport terms which integrate to zero over the entire roll, provided no energy is transported out the top.

The term in the second line of (4.10) represents the exchange in energy between the rolls and the small-scale turbulence. The exchange terms can be rewritten, after averaging individually in the x direction, to give

$$\begin{aligned}&(v'^2)_r\frac{\partial v_r}{\partial y}+(w'^2)_r\frac{\partial w_r}{\partial z}+(v'w')_r\frac{\partial v_r}{\partial z}+(v'w')_r\frac{\partial w_r}{\partial y}\\ &+(u'v')_r\frac{\partial u_r}{\partial y}+(u'w')_r\frac{\partial u_r}{\partial z}+(u_i'u_j')_r\frac{\partial u_i''}{\partial x_j},\end{aligned} \tag{4.11}$$

where the double prime terms represent interaction with kilometer-scale turbulence [see (4.4)].

The first four of these terms appear with opposite sign in LeMone's (1972) equation for roll energy at a point:

$$\begin{aligned}\frac{\partial E_r}{\partial t}=&-v_rw_r\frac{d\bar{V}^*}{dz}+\frac{g}{\bar{T}}w_rT_r^*-fu_rv_r\\ &+\tilde{f}u_rw_r\cos\phi-u_{ri}\frac{\partial}{\partial x_i}(u_i''u_j'')(1-\delta_{i1})\\ &-\frac{\partial}{\partial x_i}[v_r(u_i'v')_r+w_r(u_i'w')_r](1-\delta_{i1})\\ &\quad\text{EX1}\qquad\text{EX2}\qquad\text{EX3}\qquad\text{EX4}\\ &+\left[(v'^2)_r\frac{\partial v_r}{\partial y}+(w'^2)_r\frac{\partial w_r}{\partial z}+(v'w')_r\frac{\partial v_r}{\partial z}+(v'w')_r\frac{\partial w_r}{\partial y}\right]\\ &-\left[\frac{1}{\bar{\rho}}\frac{\partial}{\partial y}(p_rv_r)+\frac{1}{\bar{\rho}}\frac{\partial}{\partial z}(p_rw_r)+\frac{\partial}{\partial y}(v_rE_r)\right.\\ &\left.+\frac{\partial}{\partial z}(w_rE_r)+\bar{V}\frac{\partial E_r}{\partial y}\right].\end{aligned} \tag{4.12}$$

The two terms which describe the interaction with u_r do not appear in (4.12) because of the definition of roll energy at a point as $\frac{1}{2}(v_r^2+w_r^2)$. The first set of terms in brackets in (4.12), which also represents energy exchange between the rolls and turbulence, will integrate to zero over the entire roll circulation, provided the flux of energy out the top is zero. *Under these restrictions, the interaction between small-scale turbulence and rolls, integrated over the roll circulation, is described by terms EX1 through EX4, integrated over the same volume.*

The terms with asterisks in (4.12) are those found by LeMone (1973) to be important in the production and maintenance of the observed rolls. The exchange terms will be evaluated and compared to the larger of these two terms, the buoyancy term, in the next section. Note that in the Coriolis term, $\tilde{f}u_rw_r\cos\phi$, first included in the roll stability equation by Etling (1971), $\tilde{f}$ is the horizontal component of the Coriolis parameter and ϕ the angle of the rolls with respect to east.

5. The physics of the modulation and its relationship to roll maintenance

Using the data discussed in Section 3 in the roll-modulated turbulence energy equation (4.10) from Section 4, we will first determine the physical mechanisms most important in maintaining the systematic modulation of turbulence, and then discuss the importance of the modulation in the roll energy equation (4.12).

TABLE 1. Terms (ergs g^{-1} s^{-1}) in the roll-modulated turbulence energy budget (4.10) for 1 October 1970, evaluated at maximum and minimum roll vertical velocity.

	Height 46 m (6 rolls) max w_r	46 m (6 rolls) min w_r	110 m (3 rolls) max w_r	110 m (3 rolls) min w_r	175 m (3 rolls) max w_r	175 m (3 rolls) min w_r
$-(u'w')_r\frac{d\bar{U}^*}{dz}$	44	26	64	4	13	−2
$(w'T_v')_r\frac{g}{T_v}$	50	50	57	20	76	64
$-w_r\frac{\partial(E')_r}{\partial z}$	−2	−8	−4	−21	−7	−38
$-(w'^2)_r\frac{\partial w_r}{\partial z}$	−35	−31	−79	−33	−61	−16
$-(v'^2)_r\frac{\partial v_r}{\partial y}$**	36	32	69	24	43	8
$-(v'^2)_r\frac{\partial v_r}{\partial y}$	14	13	31	11	34	6

* $d\bar{U}/dz$ assumed equal to u_*/kz, u_* assumed constant.
** $\partial v_r/\partial y$ set equal to $\partial w_r/\partial z$ [see (4.8)].

a. *Evaluation of terms*

It is possible to estimate most of the production, divergence, and roll-turbulence interaction terms of (4.10) for the three cases for which the Buffalo aircraft collected data. We noted earlier that the small number of rolls sampled led to some irregularity in the composite curves (such as those in Figs. 6–8) from which the calculations are made. These irregularities are removed by approximating each curve by a best fit sine curve in phase with the roll vertical velocity w_r. Only the triple-correlation terms of the form $(a'b'^2)_r$ were too irregular to justify approximation. Turbulent-triple correlations, roll-modulated dissipation, pressure transport terms, and production of turbulence energy from cross-roll shear, $\overline{dV}/dz$ (assumed small), will not be considered here.

TABLE 2. As in Table 1 except for 5 November 1970.

	Height 30 m (2 rolls) max w_r	30 m (2 rolls) min w_r	110 m (2 rolls) max w_r	110 m (2 rolls) min w_r	320 m (3 rolls) max w_r	320 m (3 rolls) min w_r
$-(u'w')_r\frac{d\bar{U}^*}{dz}$	78	−57	2	−7	10	1
$(w'T_v')_r\frac{g}{\bar{T}_v}$	data scattered; amplitude of modulation small					
$-w_r\frac{\partial(E')_r}{\partial r}$	0.3	−0.2	1	−1	1	−0.4
$-(w'^2)_r\frac{\partial w_r}{\partial z}$	−4	3	−2	1	0	0
$-(v'^2)_r\frac{\partial v_r}{\partial y}$**	5	−4	2	−1	0	0
$-(v'^2)_r\frac{\partial v_r}{\partial y}$	1	−1	2	−1	0	0

* $d\bar{U}/dz$ assumed equal to u_*/kz at 30 m; otherwise from direct measurements of wind profile.
** $\partial v_r/\partial y$ assumed equal to $\partial w_r/\partial z$ [see (4.8)].

TABLE 3. As in Table 1 except for 16 November 1970.

	60 m (7 rolls) max w_r	60 m (7 rolls) min w_r
$-(u'w')_r\frac{d\bar{U}^*}{dz}$	28	6
$(w'T_v')_r\frac{g}{\bar{T}_v}$	9	5
$w_r\frac{\partial(E')_r}{\partial z}$	insufficient data	
$-(w'^2)_r\frac{\partial w_r}{\partial z}$	−13	10
$-(v'^2)_r\frac{\partial v_r}{\partial y}$**	7	−7
$-(v'^2)_r\frac{\partial v_r}{\partial y}$	4	−3

* $d\bar{U}/dz$ assumed equal to u_*/kz.
** $\partial v_r/\partial y$ assumed equal to $\partial w_r/\partial z$ [see (4.8)].

b. *Maintenance of the modulation*

From the foregoing discussion, the maxima and minima for the modulated turbulence kinetic energy and roll vertical velocity coincide. This means that the change in the size of any term in (4.10) from minimum to maximum w_r is directly related to the change in modulated turbulence kinetic energy; that is, to the amplitude of the modulation of turbulence kinetic energy by rolls.

The turbulence production and transport terms of (4.10), evaluated at the points at which the roll vertical velocity is maximum or minimum, appear in Tables 1–3. We note that the modulation is maintained by the variation across the roll of buoyancy production, $(w'T_v')_r(g/\bar{T}_v)$; shear production from the large scale mean flow, $(u'w')_r(d\bar{U}/dz)$; vertical transport of turbulence energy by the roll, $w_r[\partial(E')_r/\partial z]$; and the roll turbulence interaction term, $-(v'^2)_r(\partial v_r/\partial y)$.

The relative importance of the production and transport terms varies with height in a way similar to their analogues in the turbulence energy budget, as reported by Lenschow (1970) and Pennell and LeMone (1974).[4]

[4] Both Lenschow (1970) and Pennell and LeMone (1974) documented the decrease with height of turbulence energy production through the mixed layer. Noting the increase in scale of the maximum eddy energy with height (see Bean *et al.*, 1972), we would expect the production of energy by smaller scale turbulence to decrease even faster.

Nearer the surface, but high enough so that the modulation is established, the local production of energy by shear from the mean flow, and buoyancy production are important. Here, vertical transport of energy by the roll vertical velocity is still small or may even tend to reduce the modulation. [The quantity $\partial(E')_r/\partial z$ may be positive at maximum w_r if the amplitude of the modulation increases sufficiently fast with height to counteract the normal decrease with height of $\overline{E}'$.]

Tables 1 and 2 show that the vertical transport of turbulence energy by the roll is more important in maintaining the modulation at greater heights. For example, at the highest level of measurement on 1 October (175 m, Table 1), the contribution of the energy transport to the modulation, with a range of 31 ergs g^{-1} s^{-1} from minimum to maximum roll vertical velocity, is greater than the combined contributions of the two production terms (27 ergs gm^{-1} s^{-1}).

Of the roll-turbulence interaction terms in (4.11), the $(v'^2)_r\partial v_r/\partial y$ and $(w'^2)_r\partial w_r/\partial z$ terms are the most important. The former intensifies the modulation and the latter reduces it, with a relatively small net effect. The production of energy from the lateral shear in the roll circulation, expressed by $(v'w')_r(\partial v_r/\partial z)$, should be unimportant in the maintenance of the modulation, at least in the lower part of the roll. Here v_r and hence $\partial v_r/\partial z$ is small at both maximum and minimum w_r. The production term $(v'w')_r(\partial w_r/\partial y)$ is identically zero at these two points. LeMone (1973) notes no systematic relationship of u_r to the roll circulation, so it is difficult to assess the importance of terms containing u_r, even on an idealized basis. However, the u_r terms are probably smaller than $(w'^2)_r\partial w_r/\partial z$ and $(v'^2)_r\partial v_r/\partial y$ since the former terms contain the cross-correlation factors $(u'v')_r$ and $(u'w')_r$.

The terms tending to reduce the amplitude of the modulation are obviously not well represented in Tables 1–3. Only the roll-turbulence interaction term involving $(w'^2)_r$ tends to oppose the modulation. Perhaps more important in reducing the amplitude of the turbulence modulation, by analogy with the total turbulence energy budget, would be the dissipation and pressure terms of (4.10). Wyngaard and Coté (1971) report that both terms may be significant in balancing the production terms in the surface layer, while both Lenschow (1970) and Pennell and LeMone (1974) show dissipation to be the major sink of turbulence energy throughout the mixed layer.

TABLE 4. Energy exchange (ergs g^{-1} s^{-1}) between rolls and roll-modulated turbulence. Terms are positive if energy is passed from turbulence to the rolls.

Height (m)	$\overline{(w'^2)_r\frac{\partial w_r}{\partial z}}$	$\overline{(v'^2)_r\frac{\partial v_r^*}{\partial y}}$	$\overline{(v'^2)_r\frac{\partial v_r}{\partial y}}$	Sample size
Haswell, Colorado, 1 October 1970				
46	1	−1	0	6 rolls
110	12	−11	−5	3 rolls
175	11	−9	−7	3 rolls
Lake Michigan, 5 November 1970				
33	0.1	−0.3	−0.1	2 rolls
110	0.2	−0.1	−0.1	2 rolls
320	0	0	0	3 rolls
Lake Michigan, 16 November 1970				
60	0.7	−0.2	−0.2	7 rolls

* $\partial v_r/\partial y$ assumed equal to $\partial w_r/\partial z$ [see (4.8)].

c. *The exchange of energy between rolls and smaller scale turbulence through modulation*

The energy exchanged between two-dimensional rolls and small-scale turbulence, under the assumption stated earlier, are given by the four terms

$$(v'^2)_r\frac{\partial v_r}{\partial y}+(w'^2)_r\frac{\partial w_r}{\partial z}+(v'w')_r\frac{\partial w_r}{\partial y}+(v'w')_r\frac{\partial v_r}{\partial z} \quad (5.1)$$

integrated over the depth of the roll. From (4.10) and (4.12), the energy flow is from rolls to turbulence if the terms are negative, and from turbulence to rolls if the terms are positive. Note that it is the amplitude of the modulation, rather than the average turbulence intensity, that actually determines the size of the energy exchange. Averaging the first term in (5.1) in the y direction, for example, we obtain

$$\overline{(v'^2)_r\frac{\partial v_r}{\partial y}}=\overline{(v'^2)_r^m\frac{\partial v_r}{\partial y}}+\overline{\overline{(v'^2)}_r\frac{\partial v_r}{\partial y}}=\overline{(v'^2)_r^m\frac{\partial v_r}{\partial y}}, \quad (5.2)$$

where the terms with the m superscripts represent the departure from the mean owing to the modulation. These terms fluctuate sinusoidally about a zero mean across the roll. The third term in (5.2) is identically zero because $\partial v_r/\partial y$ is zero.

The first two terms of (5.1) are evaluated for the three cases in Table 4. It is clear that $(w'^2)_r\partial w_r/\partial z$ passes energy from the turbulence to the rolls, while $(v'^2)_r\partial v_r/\partial y$ passes energy from the rolls to the turbulence. The net result, whether calculated directly or by substituting $-\partial w_r/\partial z$ for $\partial v_r/\partial y$,[5] is a small net gain of energy by the rolls. We note, by combining these two terms under the assumption of two-dimensional continuity [Eq. (4.8)], that

$$\overline{(v'^2)_r\frac{\partial v_r}{\partial y}}+\overline{(w'^2)_r\frac{\partial w_r}{\partial z}}=\overline{[(w'^2)_r-(v'^2)_r]\frac{\partial w_r}{\partial z}}. \quad (5.3)$$

Thus, in the lower part of the roll, the energy will pass

[5] Since the compositing with respect to w_r tends to emphasize $\partial w_r/\partial z$ and to smear out $\partial v_r/\partial y$, this is probably the better procedure.

to the roll if $(w'^2)_r$ fluctuates with greater amplitude than $(v'^2)_r$.

The mechanical production from roll shear is given by the two $(v'w')_r$ terms in (5.1). The net contribution of these terms at a given level is probably small compared to that of either of the first two terms of (5.1), since $(v'w')_r$ is close to 90° out of phase with $\partial w_r/\partial y$ and $\partial v_r/\partial z$, and $(v'w')_r$ is small compared to $(v'^2)_r$ and $(w'^2)_r$. If the turbulence modulation is exactly in phase with w_r, as assumed here, one of these two terms, $(v'w')_r(\partial w_r/\partial y)$, will average to zero across the roll.

For the cases examined, the contribution of the four exchange terms to the roll energy budget is much smaller than that of buoyancy. From Fig. 5, the roll energy derived from buoyancy at 100 m is 23 ergs g^{-1} s^{-1} and 1.4 ergs g^{-1} s^{-1} over Haswell and Lake Michigan, respectively. The sum of the dominant $(v'^2)_r\partial v_r/\partial y$ and $(w'^2)_r\partial w_r/\partial z$ exchange terms at 100 m is between 5 and 10 ergs g^{-1} s^{-1} over Haswell and 0.1–0.2 erg g^{-1} s^{-1} over Lake Michigan. The Haswell observations were made on a clear day with strong winds, with strong heat flux at the surface. Under similar conditions, LeMone (1973) documented roll buoyancy positive for at least the lower 80% of the roll. However, the dominant exchange terms will become smaller, and possibly negative above $0.33z_I$ (z_I is the depth of the roll), since the intensity of small-scale turbulence decreases with height up to near the top of the roll, and w_r is smaller in the upper part of the roll. It is likely that the mechanical production terms of (5.1) are both smaller and opposite in sign over much of the roll depth. Hence it can be tentatively concluded that the contribution of turbulence modulation to the roll energy budget is rather small.

A more important, disruptive effect on the rolls would be through the double-primed terms in (4.12). These could become large if, for example, a field of plumes became sufficiently strong to frequently penetrate into the negative roll vertical velocity region. When the rolls coexist with cells, as observed by Konrad (1970), the effects of the cells are also felt through the double-primed terms.

6. Summary and conclusions

Superimposed on the mean circulation of horizontal roll vortices in the thermally unstable planetary boundary layer is high-frequency turbulence of varying intensity, with small-scale variances and fluxes systematically concentrated in the positive vertical velocity regions of the rolls. This turbulence modulation is the result of the redistribution of turbulence-producing elements by the roll mean circulation. Near the surface, the roll lateral velocity v_r transports the elements horizontally into regions of upward vertical velocity. Here the elements are transported upward; or, if the elements are plumes, they grow upward at an accelerated rate.

There is little energy exchange between the smaller scale turbulence and the rolls associated with this modulation. Rather, the modulation of small-scale turbulence by the rolls is maintained chiefly by terms like those which are important in the turbulence kinetic energy budget of a typical unstable boundary layer. Nearer the surface the variation of turbulence kinetic energy across the roll is mainly the result of the variation in shear production from the mean flow and in buoyancy production. At a higher level the vertical transport of turbulence kinetic energy by the roll increases in importance. At all heights varying dissipation rates probably tend to even out the distribution of turbulence, reducing the modulation. The effects of the roll-turbulence interaction terms almost cancel, with a combined amplitude much smaller than that of the other terms. Similarly, the interaction terms are negligible in the roll energy equation, being an order of magnitude smaller than the buoyancy term.

Acknowledgments. The author is indebted to Drs. R. G. Fleagle, R. A. Brown, J. A. Businger and D. H. Lenschow, for their many valuable suggestions during various phases of this research. Support during the course of this work was supplied by an NDEA Title IV Fellowship, the National Center for Atmospheric Research, the National Severe Storms Laboratory, and the Energy Transfer Group of the Department of Atmospheric Sciences at the University of Washington, which is funded by the National Science Foundation under Grant GA31317X.

APPENDIX

Table of Symbols

E'	turbulence-scale kinetic energy $[=\frac{1}{2}(u'^2+v'^2+w'^2)]$
E_r	kinetic energy of two-dimensional rolls $[=\frac{1}{2}(v_r^2+w_r^2)]$
f_c	cutoff frequency (Hz) in Eqs. (2.1) and (4.5)
f_t	terminating frequency where response function of the filter in (2.1) goes to zero
g	acceleration of gravity (9.8 m s^{-2})
L	Obukhov length
p	pressure
q	any (scalar) quantity
$\bar{Q}$	average of $q\left[=\frac{1}{N}\sum_{i=1}^{N} q_i\right]$
q_l	fluctuations in q of scales of the order of 500 m to a few kilometers, found from applying a low-pass filter [(2.1)] to $q-\bar{Q}$ [see (2.2) and (4.3)]
q'	fluctuations in q of scales smaller than ~500 m to kilometer scale [see (2.2) and (4.3); examples are plumes and turbulence eddies]

q_r fluctuations of q associated with idealized two-dimensional rolls [see (2.3) and (4.4)]

q'' kilometer-scale fluctuations not associated with idealized, two-dimensional rolls [examples are fluctuations associated with large thermals or convection cells; see (4.4)]

$(q'^2)_r$ Roll-modulated turbulence variance of q found by
Subtracting $q_l+\bar{Q}$ from q to obtain q' [see (2.2)].
Squaring q' at each point, to obtain q'^2.
Filtering the time series q'^2, using the filter (2.1), to obtain $(q'^2)_l$.
Compositing, that is, averaging $(q'^2)_l$ at corresponding points of several rolls to obtain $(q'^2)_r$ [see (2.3)].

T temperature (K)

T_v virtual temperature (K)

u_* the square root of the total momentum flux magnitude at the surface

$$\{=[\overline{(u_l+u')(w_l+w')}^2+\overline{(v_l+v')(w_l+w')}^2]_0^{\frac{1}{2}}\}$$

u component of wind along roll axis, positive downwind (m s^{-1})

v component of wind normal to roll axis, positive to left, looking downwind (m s^{-1})

$\mathbf{V}$ $[=u\mathbf{i}+v\mathbf{j}+w\mathbf{k}]$

w component of wind normal to roll axis, positive vertically upward (m s^{-1})

x, y, z distance along axis of right-handed Cartesian coordinate system whose x axis points downwind along the roll axis

ϵ turbulence dissipation

ρ_v water vapor density (gm m^{-3})

$\mathbf{\Omega}$ earth's rotation vector

REFERENCES

Asai, Tomio, 1970: Stability of plane parallel flow with variable vertical shear and unstable stratification. *J. Meteor. Soc. Japan*, **48**, 129–139.

Bean, B. R., R. Gilmer, R. Grossman, R. McGavin and C. Travis, 1972: An analysis of airborne measurements of vertical water vapor flux during BOMEX. *J. Atmos. Sci.*, **29**, 860–869.

Brown, R. A., 1970: A secondary flow model for the planetary boundary layer. *J. Atmos. Sci.*, **27**, 742–757.

Charnock, H., 1957: Notes on the specification of atmospheric turbulence. *Proc. Roy. Statist. Soc.*, **A164**, 231–232.

Etling, D., 1971: Einfluss der thermischen Schichtung auf die Stabilität einer Ekman'schen Grenzschichtstromung. *Beitr. Phys. Atmos.*, **44**, 168–186.

Faller, A. J., and R. E. Kaylor, 1966: A numerical study of the laminar Ekman layer. *J. Atmos. Sci.*, **23**, 466–480.

Fleagle R. G., 1972: BOMEX: An appraisal of results. *Science*, **172**, 1079–1084.

Friedman, H., G. Conrad and J. McFadden, 1970: ESSA Research Flight Facility aircraft participation in BOMEX. *Bull. Amer. Meteor. Soc.*, **51**, 822–834.

Graham, R. J., 1963: Determination and analyses of numerical smoothing heights. NASA Tech. Rept. TR-179, Office of Technical Services, Dept. of Commerce, Washington, D. C.

Haugen, D. A., J. C. Kaimal and E. F. Bradlay, 1971: An experimental study of Reynolds stress and heat flux in the atmospheric surface layer. *Quart. J. Roy. Meteor. Soc.*, **97**, 168–180.

Holland, J. Z., 1973: A statistical method for analyzing wave shapes and phase relationships of fluctuating geophysical variables. *J. Phys. Oceanogr.*, **3**, 139–155.

Konrad, T. G., 1970: The dynamics of the convective process in clear air as seen by radar. *J. Atmos. Sci.*, **27**, 1138–1147.

Kuettner, J. P., 1971: Cloud bands in the earth's atmosphere: Observations and theory. *Tellus*, **11**, 267–294.

LeMone, M. A., 1972: The structure and dynamics of the horizontal roll vortices in the planetary boundary layer. Ph.D. dissertation, University of Washington, 128 pp.

——, 1973: The structure and dynamics of horizontal roll vortices in the planetary boundary layer. *J. Atmos. Sci.*, **30**, 1077–1091.

Lenschow, D. H., 1970: Airplane measurements of planetary boundary structure. *J. Appl. Meteor.*, **9**, 874–884.

——, 1972: The measurement of air velocity and temperature using the NCAR Buffalo aircraft measuring system. NCAR-TN/EDD-74, National Center for Atmospheric Research, 39 pp.

Lilly, D. K., 1966: On the stability of Ekman boundary flow. *J. Atmos. Sci.*, **23**, 481–494.

——, and D. H. Lenschow, 1974: Aircraft measurements of the atmospheric mesoscales using an inertial reference system. *Proc. First Symp. on Flow, its Measurement and Control in Science and Industry*, Inst. Soc. Amer., Pittsburgh, Pa., 369–377.

Pennell, W. T., and M. A. LeMone, 1974: An experimental study of turbulence structure in the fair-weather trade wind boundary layer. *J. Atmos. Sci.*, **31**, 1308–1323.

Wyngaard, J. C., and O. R. Coté, 1971: The budgets of turbulent kinetic energy and temperature variance in the atmospheric surface layer. *J. Atmos. Sci.*, **28**, 190–201.